2.6 Ionization

2.6.1 Introduction and general description

General aspects of the ionization of neutral atoms by electron impact have been summarized in a number of reviews [71Ino1] and books [85Mär1]. Some surveys of the electron impact ionization data have been reported in several compilations [83Bel1, 87Taw1, 88Len1, 89Hig1] as well as in several databases (for example, NIFS [www1], JAERI [www2], ORNL [www3] and IAEA [www4]) from where relevant numerical as well as bibliographic data can be retrieved electronically.

The apparent ionization cross sections,

$$\sigma_i^a = \sum_m m\sigma_i^{m+} \quad (m \text{ is the charge state of the product ions}),$$

for most of the neutral atoms can be determined with reasonably good accuracies by crossing the energy-selected incident electrons through the gas targets and, then, measuring the secondary electrons or ions with a pair of the parallel plates, except for elements such as high melting materials which can not be easily evaporated and are hard to determine their absolute densities. Such neutral atom targets can be prepared via the electron capture into the parent ions and, then, the ionization cross sections can be determined through so-called crossed-beams technique where the target atoms cross the mono-energetic incident electrons and the product ions are charge-analyzed to determine the intensities of ions with different charges. However, it should be kept in mind that the neutral atoms prepared in such ways often include a significant fraction of the excited or metastable state beams which strongly influence the observed ionization cross sections.

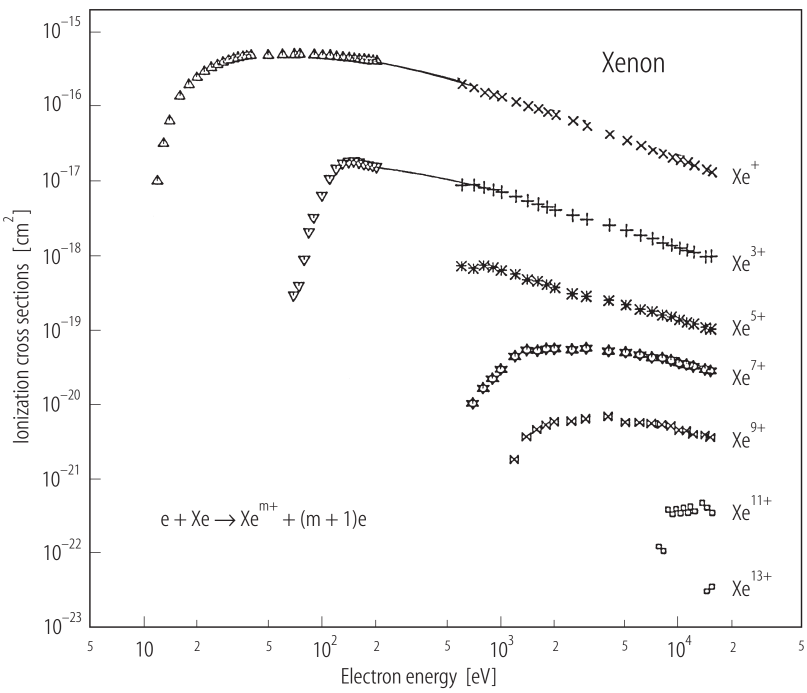

Fig. 2.6.1. Electron impact ionization cross sections for various ionization states of Xe^{m+} (m = 1, 3, 5, 7, 9, 11, 13) ions from neutral Xe atoms as a function of the electron impact energy. The solid lines are given to guide eyes (The data are taken from our database at NIFS).

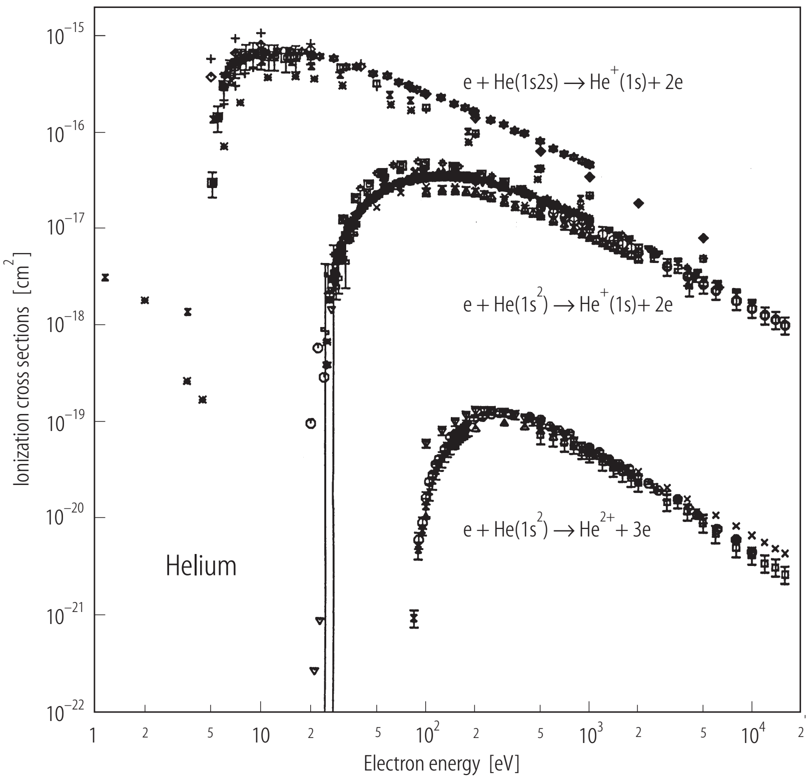

Fig. 2.6.2. Comparison of single-electron ionization cross sections for the ground and metastable He atoms under electron impact, together with those for double-electron ionization of the ground state helium atoms.

Another technique such as a time-of-flight spectrometer or magnetic analyzer is required to get the partial ionization cross sections (σ_i^{m+}) for ions with different charge states (m). Typically, as the the number of the electrons to be ionized (m) increases, the cross sections decrease drastically due to the increased binding energy, as shown in Fig. 2.6.1 where the observed cross sections of the production of multiply ionized Xe^{m+} (m = 1…13) ions from neutral Xe atoms under the single collisions of electron impact are given as a function of the electron impact energy.

Usually the metastable state beams have very large cross sections as well as the lower ionization threshold energy. In Fig. 2.6.2 is shown a comparison of the ionization cross sections for the ground $He(1s^2)$ and metastable $He(1s2s\ ^3S)$ atoms under electron impact which are prepared via electron capture into He^+ ions passing through gas targets. It is worth to note that the agreement among different experiments seems to be reasonably good for the metastable state helium atoms. Clearly the observed curve for the metastable state helium atoms shows the lower threshold energy and their cross sections are much larger than those for the ground state. Also the double-electron ionization cross sections into He^{2+} ions from the ground state He atoms are also compared in this figure.

2.6.2 Experimental techniques for neutral atom targets

2.6.2.1 Orthodox method

Here is some short description of experimental techniques relevant to the ionization of neutral atoms under electron impact. Measurements of the ionization cross sections of neutral gas atoms by electron impact are relatively simple. There are some good reviews on the ionization phenomena by electron impact and the most important aspects of these processes have been summarized [85Mär1]. So-called condenser-plate techniques can provide reliable apparent total ionization cross section, namely $\sum_m m\sigma_i^{m+}$, with the accuracies of 2…3 % [86Be1]. The partial ionization cross section for each m-electron ionization state, σ_i^{m+}, should be determined through separately measuring the relative fractions of ions in different charge states, for example by the time-of-flight techniques [87Sha1] or magnetic analyzers, and then by normalizing them to the apparent total ionization cross sections.

2.6.2.2 Magneto-optically trapped targets

This is a new technique to determine the ionization cross sections without knowing the absolute target densities. In the magneto-optical trap (MOT), the quadrupole magnetic field is shaped to be zero at the center of the trap where the laser force traps atoms at the room temperature, cool down to 100 μK and confine them to the size of a half mm with the density of about 10^6 atoms/cm^3. Then, the trapping magnetic and laser fields are switched off and the target atoms are stabilized to the ground state and the electron beam is sent into a ball of the the target atoms which are ionized. Now the trapping fields are restored where the ionized ions can leave the trapping, meanwhile the non-ionized atoms are once again retrapped and recooled down. The absolute ionization cross sections can be determined through the loss rate measurements of the trapped atoms and the accurate knowledge of the electron beam density distributions over the target. The most important merit of this method is the fact that no absolute target density is required to know. The observed cross sections represent the total ionization cross section, namely $\sum_m \sigma_i^{m+}$ (Note that "total cross section" is different from "apparent cross section" obtained through the parallel plate technique mentioned above). The accuracies are estimated to be roughly 10 %, depending slightly upon the collision energy, which comes mostly from the escape loss of the recoiling atoms from the shallow trap [96Sch1].

2.6.2.3 Excited species targets

In many applications, the excited neutral species, in particular those in the metastable states, are known to play an important and critical role [92Tra1, 96Tan1]. Therefore, it is necessary to have the reliable ionization data for such species. It is natural to expect that the cross sections for such excited species are quite large, compared with those in the ground state species. Therefore, even a very small fraction of such excited species in the target significantly influence the observed results. Unfortunately, it is not easy to get such species (specified in its electronic states) prepared with sufficient intensities under the controlled conditions. As shown in Fig. 2.6.2 (Subsect. 2.6.1), the metastable He(1s2s ^{3}S) atoms have been investigated by different authors using the crossed-beams technique and the observed cross sections show relatively good agreement with each other. Here He(1s2s ^{3}S) atoms are produced through the electron capture into He^+ ions.

Only a limited number of the experiments have been performed for some species, such as alkali or alkaline metal targets, using the three (electron + ground state species + laser)-beams crossed technique in combination with the laser excitation. Some detailed description of the important aspects of the preparation (gas-discharge, electron beam impact, electron capture, laser excitation), detection, target density determination and comparison of the relevant cross sections over the ground state has been given [92Tra1]. It should also be noted that their production efficiencies are generally quite small and, thus, the densities of the excited species target are small, compared with those for the background gas atoms.

Indeed the absolute density determination of the excited state species is one of the most difficult tasks in measurements of the collision cross sections. The laser-based technique for the excitation of the target atoms including the species with the short life-time should be the most reliable and possible to get relative high efficiencies but the present-day lasers are still limited in applications only to alkali or alkaline metal atoms [93Gie1, 93Ric1, 97Dep1]. Also it is not straightforward to define the electronic states and the fractions in the product beams which often include some different electronic configurations, except for some neutral beam with a single metastable state.

Furthermore, in combination of a series of the lasers with different wave-lengths in multi-step excitation processes, it is possible to get quite pure excited species even in very high Rydberg states such as n = 10 where the collision cross sections can be as large as 10^{-11} cm^2 [95DeP1]. The metastable beam targets such as He*(1s2s) can be obtained through the electron capture into the proper ions such as He^+ ions and have been used in the crossed-beams technique. One of typical cross sections for the metastable He(1s2s) beam is already shown in Fig. 2.6.2, compared with those for the ground state $He(1s^2)$ beam.

In Table 2.6.1 are shown the metastable state species of rare gas atoms and their features.

Table 2.6.1. Energies and lifetimes of the metastable states of rare gas atoms [92Tra1].

Atom	Term	Energy [eV]	Lifetime [s]
He	$2\ ^3S_1$	19.82	$6{\cdot}10^5$
	$2\ ^1S_0$	20.61	$2{\cdot}10^{-2}$
Ne	$3\ ^3P_2$	16.62	≈ 1
	$3\ ^3P_0$	16.72	≈ 1
Ar	$4\ ^3P_2$	11.55	≈ 1
	$4\ ^3P_0$	11.72	≈ 1
Kr	$5\ ^3P_2$	9.92	≈ 1
	$5\ ^3P_0$	10.56	≈ 1
Xe	$6\ ^3P_2$	8.32	-
	$6\ ^3P_0$	9.45	-

2.6.3 Contribution of various processes to ionization

Not only the *direct* ionization processes in neutral atoms where some electrons in the outermost-shell as well as in the inner-shell are directly removed from the target but also the *indirect* ionization processes following the innershell excitation processes play a role in the overall ionization processes and related fields. In some electronic configurations of the target ions as will be shown in Section 3.2, the contribution of the indirect ionization processes to total ionization becomes far more significant and often are more important than that of the direct processes.

2.6.3.1 Direct processes

In simple atomic targets, the contribution to the ionization dominantly comes from so-called *direct ionization* (*DI*) process where m electrons are ionized under electron impact as expressed as follows:

$$e + A \rightarrow e + A^{m+} + me. \tag{1}$$

Also it should be noted that not only a single electron (m = 1) but also two electrons (m = 2: double ionization) can be ionized simultaneously with relatively high probabilities. The single-electron ionization cross sections are generally larger than those of double- or multiple-electron ionization, as seen in Fig. 2.6.1.

As the electron impact energy increases, some of the innershell electrons can be ionized. As the energy required to ionize the inner-shell electron is larger than that for the outermost-shell electron, the cross sections usually show some shoulders at the threshold energy of the inner-shell electron ionization, in addition to the first threshold due to the ionization of the outermost-shell electron when the cross sections are plotted as a function of the electron impact energy. A typical example of the contribution of the (4d) innershell-electron ionization is compared with that of the (5s+5p) outer-shell-electron ionization in Fig. 2.6.3 where the single-electron ionization from six 5p-shell or two 5s-shell electrons results in Xe^{+} ions from Xe atoms.

Also a further deep innershell-electron ionization results mostly in the production of multiple-electron ionization through cascading processes. Among multiple ionization, the double-electron ionization (m = 2) processes are usually dominant over higher ($m \geq 3$) ionization processes and can contribute significantly to the total ionization (more than 30 % in Xe atom ionization).

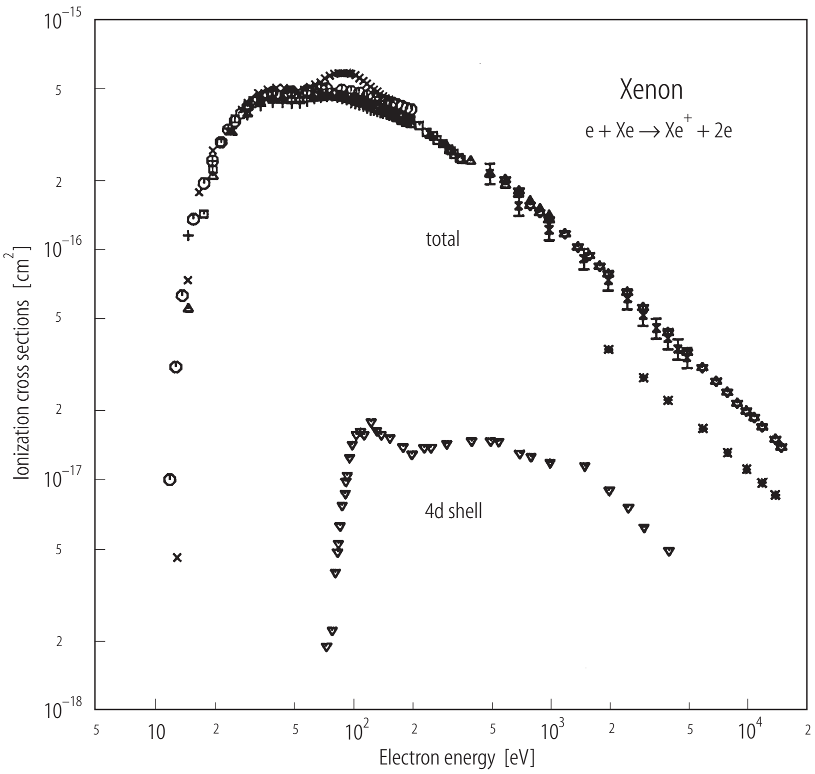

Fig. 2.6.3. A typical example of the contribution of the outer (5p+5s)- and inner (4d)-shell electron ionization of Xe atoms resulting in Xe^{+} ions under electron impact. The upper curve represents the total single-electron ionization cross sections and the lower curve corresponds to the 4d-shell electron ionization.

2.6.3.2 Indirect processes

But in many-electron targets, the significant contribution often comes from so-called indirect processes which involve the innershell electrons. After one of the inner-shell electrons is excited under the incident electron impact, the doubly or triply excited states are formed which decay through the secondary (as well as ternary) processes such as the autoionization processes and finally are stabilized into the ground state of highly ionized ions.

There are a number of different types of the indirect processes. In ionization of neutral atoms, the most significant is the innershell-electron excitation followed by autoionization (EA) process where one of the inner-shell electrons in a target atom is first excited above the threshold of the ionization limit of singly-charged ions, forming the intermediate doubly excited states, a part of which are stabilized though the autoionization process:

$$e + A \rightarrow e + A^{**} \rightarrow e + A^{+} + e. \quad (2)$$

The rest is the simple excitation process and stabilized through radiative emission which does not contribute to the ionization. The double ionization processes can also be contributed by similar indirect processes mentioned above.

2.6.4 Recommended ionization cross sections for neutral atoms

2.6.4.1 General features of the ionization cross section behavior

The cross sections for single- as well as multiple-electron ionization have been measured for a large number of the neutral atoms, which can also be seen on databases, for example at NIFS. As mentioned in Introduction, there are some compilations and reviews of the ionization data for neutral atom targets under electron impact [83Bel1, 87Taw1, 88Len1, 89Hig1]. Table 2.6.2 shows a summary of the present situations on the electron impact ionization data of neutral atoms which are stored and available in our databases at NIFS.

These data have different degree of the accuracies. Therefore, we have to evaluate them to provide reliable cross sections of ionization for the basic research as well as applications.

Table 2.6.2. Summaries of the experimental electron impact ionization data of neutral atoms under electron impact seen in the databases at NIFS. The final charge of ions produced are shown on the abscissa (horizontal direction) for each element (the vertical direction) and the number in tables shows the number of the experimental investigations performed so far.

Atom	Final charge state												
	1+	2+	3+	4+	5+	6+	7+	8+	9+	10+	11+	12+	13+
H	8												
He	26	8											
Li	6	1											
Be	2												
B	1												
C	2												
N	3												
O	7	3											
F	1												

Atom	Final charge state												
	1+	2+	3+	4+	5+	6+	7+	8+	9+	10+	11+	12+	13+
Ne	20	14	14	5	2								
Na	3	1											
Mg	6	3	1	1									
Al	2												
Si	1	1											
P	1	1											
S	2	2											
Cl	1	1											
Ar	22	20	14	9	7	3	1						
K	3												
Ca	2	1											
Ti	1												
Cr	2												
Fe	3	1											
Ni	1												
Cu	2	2	1	1	1								
Zn	2												
Ga	4	4	3	1									
Ge	2	1	1										
As	1	1											
Se	2	1	1										
Br	1	1											
Kr	12	10	8	6	4	4	2	2	1				
Rb	1	6	1	1	1								
Sr	2	1											
Zr	1												
Mo	1												
Ru	1												
Pd	1												
Ag	3	2	1										
Cd	1												
In	3	1	1										
Sn	2	1	1										
Sb	1	1	1										
Te	2	1											
I	1												
Xe	10	9	9	5	5	3	1	1	1	1	1	1	1
Cs	1												
Ba	4	2	1	1									
Au	1												
Hg	2	1	1	1	1								
Tl	2	1											
Pb	3	3	2										
Bi	1	1	1										
U	1	1	1	1									

Evaluation of experimental data

In evaluating experimental data of absolute ionization cross sections in electron impact, the following issues are the most important and not only the data but also the experiments themselves should be closely scrutinized [97Taw1]:

(1) primary electron beam, (2) target species, (3) collision product and (4) detection system. There are a number of critical issues in each, as shown in Table 2.6.3. Unfortunately very few papers published have discussed the details on such issues and the access to the details is sometimes difficult. The most important but often neglected issue is the contribution of the excited or metastable state target species with relatively high internal energy. Though most of the target gases evaporated in high temperature ovens are in the ground state, the internal energy of the target atoms is critical in ionization processes, for example, in crossed-beams experiments where the neutral target atoms are formed through electron capture into charged particles. The ionization cross sections for such atoms are often much larger than those for the ground state species. Therefore, the excited states (nl) of the colliding neutralized beams have to be specified and and their fractions have to also be known accurately. Otherwise, the observed cross sections would be largely scattered.

Sometimes the observed cross sections have been, for simplicity, normalized to some known (previously observed, calculated or scaled) values. For example, the experimental cross sections for atomic hydrogens, due to difficulties in preparing the targets and in determining the absolute densities, are often normalized to those at high energies where the Born or other approximations can be assumed to be valid. In such a case, it should be noted that, if the collision energy is not sufficiently high, the Born approximations fail to give the exact values.

Table 2.6.3. Critical issues in evaluating experimental ionization cross sections in electron impact.

	Critical issues	Comments
Primary electron beam	kinetic energy spread	important in resonance observation
	beam focusing and divergence	transmission through apertures
	edge scattering	straying electrons produced
	external field	deflection of low energy beam
Target beam	contamination and residual gases	water vapor often included in gas line
	purity	high purity target gases available
	effective target density	due to diffusion through apertures
	beam overlapping with electrons	important at low energies
	internal energy or excited state	very critical in neutralized target atoms
Products	product specification	mass/charge
	collection and transmission efficiencies	discrimination in collecting system
	single collisions	correction to double collisions
	recoil/dissociation energy	loss of collection
	internal energy	
	life-time	loss of detection
	external field	charge discrimination
Detection	absolute detection efficiencies	or normalized to others
	pulse-height distributions	noise-discrimination
	secondary particle emission	spurious counting
	uniform sensitivities	detector with large area
	sensitivities to strayed particles	strayed photons or electrons
	reflection from surfaces	loss of particles

Evaluation of theoretical data

Some theoretical calculations are requisite when no experimental data are available. There are some critically important issues in evaluating the calculated cross sections. Indeed it is sometimes quite difficult to know if they are properly treated in references (see Table 2.6.4).

Table 2.6.4. Important issues in evaluating the calculated cross sections under electron impact.

Critical issues	Comments
approximation	Born, distorted-wave, close-coupling, R-matrix etc.
wave-function	distorted wave-function? electron correlation included?
interaction potential	simple electrostatic potential, exchange or distorted potential ?
number of states	not always accurate even for a large number of states considered
continuum states	quasi-continuum
validity (energy) region	limited energy region

Following some criterions as shown in Tables 2.6.3 and 2.6.4, the experimental *single-electron* ionization cross sections for a series of the ground state neutral species ranging from hydrogen to uranium atoms have been evaluated and listed in Table 2.6.5 (for neutral atoms ranging from H to Ne), Table 2.6.6 (Na-Ca), Table 2.6.7 (Sc-Zn), Table 2.6.8 (Ga-Zr), Table 2.6.9 (Mo-Xe) and Table 2.6.10 (Cs-U) as a function of the electron impact energy. It should be noted that, as the smooth variation of the cross sections as a function of the electron impact energy is assumed, some structures are not clearly seen in the present tables.

The smoothed data are also shown in Fig. 2.6.4 (H-B), Fig. 2.6.5 (C-Ne), Fig. 2.6.6 (Na-P), Fig. 2.6.7 (S-Ca), Fig. 2.6.8 (Sc-Mn), Fig. 2.6.9 (Fe-Zn), Fig. 2.6.10 (Ga-Br), Fig. 2.6.11 (Kr-Zr), Fig. 2.6.12 (Mo-In), Fig. 2.6.13 (Sn-Xe) and Fig. 2.6.14 (Cs-U). Note that the smoothed data plotted in these figures may be slightly different from those in tables.

2.6.4.2 Innershell electron ionization

The ionization of an innershell electron results in the formation of an innershell hole which follows a series of cascade processes before stabilization and finally a multiply charged ion is formed in most cases. The ionization cross sections for relativistic inner-shell electrons of neutral atom targets by relativistic electron impact have been surveyed recently [85Pow1, 90Lon1].

Table 2.6.5. Recommended cross sections for single-electron ionization of neutral atoms (H-Ne) under electron impact as a function of the electron impact energy (cf. Figs. 2.6.4 and 2.6.5).

Energy [eV]	Cross section [cm^2]									
	H	He	Li	Be	B	C	N	O	F	Ne
6			1.00E-16							
8			2.80E-16							
10			3.85E-16	2.50E-17	3.00E-17					
15	9.00E-18		4.25E-16	1.43E-16	1.25E-16		1.10E-17	1.00E-17		
20	3.10E-17		4.05E-16	2.15E-16	1.91E-16	1.10E-16	4.10E-17	3.20E-17	7.50E-18	
25	4.50E-17		3.70E-16	2.43E-16	2.20E-16	1.50E-16	7.20E-17	6.00E-17	2.10E-17	
30	5.30E-17	6.50E-18	3.40E-16	2.59E-16	2.43E-16	1.80E-16	9.00E-17	7.40E-17	3.30E-17	1.00E-17
40	6.10E-17	1.75E-17	2.90E-16	2.60E-16	2.52E-16	2.10E-16	1.21E-16	1.05E-16	5.10E-17	2.30E-17
50	6.40E-17	2.30E-17	2.50E-16	2.50E-16	2.49E-16	2.25E-16	1.39E-16	1.20E-16	6.80E-17	3.00E-17
60	6.30E-17	2.90E-17	2.20E-16	2.38E-16	2.41E-16	2.30E-16	1.48E-16	1.30E-16	8.00E-17	4.30E-17
80	5.90E-17	3.50E-17	1.70E-16	2.13E-16	2.22E-16	2.30E-16	1.57E-16	1.40E-16	9.20E-17	5.80E-17
100	5.40E-17	3.65E-17	1.45E-16	1.91E-16	2.03E-16	2.15E-16	1.56E-16	1.45E-16	9.60E-17	6.80E-17
150	4.50E-17	3.65E-17	1.00E-16	1.49E-16	1.63E-16	1.85E-16	1.41E-16	1.40E-16	9.80E-17	7.50E-17
200	3.80E-17	3.45E-17	8.00E-17	1.29E-16	1.46E-16	1.60E-16	1.28E-16	1.25E-16	9.00E-17	7.40E-17
300	2.80E-17	2.80E-17	5.60E-17	9.80E-17	1.13E-16	1.30E-16	1.05E-16	9.95E-17	7.75E-17	6.50E-17
400	2.30E-17	2.35E-17	4.40E-17	8.20E-17	9.40E-17	1.10E-16	9.10E-17	8.50E-17	6.75E-17	5.70E-17
600	1.70E-17	1.75E-17	3.00E-17	6.00E-17	7.20E-17	8.50E-17	7.20E-17	6.70E-17	5.50E-17	4.50E-17
800	1.35E-17	1.45E-17	2.35E-17	4.90E-17	5.80E-17	7.20E-17	5.90E-17	5.40E-17	4.55E-17	3.80E-17
1000	1.10E-17	1.20E-17	1.90E-17	4.10E-17	4.90E-17	6.20E-17	5.00E-17	4.65E-17	3.91E-17	3.20E-17
2000	6.30E-18	7.00E-18	1.00E-17	2.40E-17	2.90E-17	3.90E-17	3.10E-17	2.80E-17	2.40E-17	1.95E-17
4000	3.50E-18	3.90E-18	5.30E-18	1.40E-17	1.70E-17	2.20E-17	1.80E-17	1.60E-17	1.43E-17	1.15E-17
6000	2.40E-18	2.75E-18	3.80E-18	1.00E-17	1.25E-17	1.55E-17	1.30E-17	1.20E-17	1.05E-17	7.80E-18
10000	1.60E-18	1.80E-18	2.45E-18	7.00E-18	8.50E-18	1.00E-17	8.50E-18	7.60E-18	7.00E-18	5.10E-18

Table 2.6.6. Recommended cross sections for single-electron ionization of neutral atoms (Na-Ca) under electron impact as a function of the electron impact energy (cf. Figs. 2.6.6 and 2.6.7).

Energy [eV]	Cross section [cm^2]									
	Na	Mg	Al	Si	P	S	Cl	Ar	K	Ca
6	1.35E-16								5.20E-16	
8	3.30E-16	8.00E-17	2.50E-16						7.90E-16	2.50E-16
10	4.35E-16	2.80E-16	5.60E-16	9.00E-17					9.00E-16	7.40E-16
15	4.75E-16	4.90E-16	9.15E-16	5.10E-16	3.00E-16	1.9E-16	5.00E-17		9.00E-16	9.50E-16
20	4.60E-16	5.25E-16	9.60E-16	6.40E-16	4.20E-16	3.3E-16	1.80E-16	6.00E-17	8.40E-16	8.90E-16
25	4.35E-16	5.10E-16	9.70E-16	6.90E-16	4.85E-16	4.0E-16	2.55E-16	1.30E-16	7.80E-16	8.20E-16
30	4.15E-16	4.80E-16	9.60E-16	7.00E-16	5.20E-16	4.2E-16	3.00E-16	1.80E-16	7.30E-16	7.30E-16
40	3.55E-16	4.30E-16	9.30E-16	6.90E-16	5.25E-16	4.4E-16	3.40E-16	2.30E-16	6.20E-16	6.10E-16
50	3.20E-16	3.85E-16	8.90E-16	6.70E-16	5.20E-16	4.4E-16	3.55E-16	2.40E-16	5.70E-16	5.20E-16
60	2.90E-16	3.40E-16	8.30E-16	6.40E-16	5.10E-16	4.5E-16	3.60E-16	2.45E-16	5.40E-16	4.60E-16
80	2.45E-16	2.85E-16	7.30E-16	5.80E-16	4.75E-16	4.3E-16	3.50E-16	2.45E-16	5.00E-16	3.80E-16
100	2.10E-16	2.40E-16	6.50E-16	5.20E-16	4.40E-16	4.2E-16	3.30E-16	2.45E-16	4.90E-16	3.20E-16
150	1.65E-16	1.80E-16	5.00E-16	4.30E-16	3.80E-16	3.7E-16	2.90E-16	2.30E-16	4.20E-16	2.30E-16
200	1.40E-16	1.30E-16	4.10E-16	3.90E-16	3.20E-16	3.3E-16	2.60E-16	2.20E-16	3.90E-16	1.80E-16
300	1.10E-16	8.50E-17	3.30E-16			2.6E-16		1.75E-16	3.10E-16	1.30E-16
400	9.00E-17	6.00E-17	2.70E-16			2.2E-16		1.40E-16	2.50E-16	1.05E-16
600	7.30E-17		2.20E-16			1.7E-16		1.05E-16	1.90E-16	7.20E-17
800	6.00E-17		1.80E-16			1.4E-16		8.60E-17	1.50E-16	5.50E-17
1000	5.20E-17		1.50E-16			1.3E-16		7.20E-17	1.30E-16	4.50E-17
2000			9.00E-17			7.6E-17		4.25E-17	7.30E-17	2.30E-17
4000						4.5E-17		2.40E-17	4.20E-17	1.30E-17
6000						3.2E-17		1.80E-17	3.00E-17	8.30E-18
10000						2.3E-17		1.15E-17	2.10E-17	5.10E-18

Table 2.6.7. Recommended cross sections for single-electron ionization of neutral atoms (Sc-Zn) under electron impact as a function of the electron impact energy (cf. Figs. 2.6.8 and 2.6.9).

Energy [eV]	Cross section [cm^2]									
	Sc	Ti	V	Cr	Mn	Fe	Co	Ni	Cu	Zn
6										
8	6.60E-16		5.20E-16		1.40E-16				9.30E-17	
10	1.35E-15	5.70E-16	1.05E-15	2.30E-16	2.70E-16	1.30E-16	2.25E-16	1.20E-16	2.10E-16	5.00E-17
15	2.10E-15	8.05E-16	1.55E-15	5.00E-16	4.60E-16	4.00E-16	4.70E-16	3.40E-16	2.83E-16	2.00E-16
20	2.25E-15	8.20E-16	1.63E-15	6.40E-16	5.00E-16	5.00E-16	5.10E-16	4.20E-16	3.10E-16	3.40E-16
25	2.20E-15	7.90E-16	1.60E-15	7.70E-16	5.05E-16	5.20E-16	5.34E-16	4.35E-16	3.13E-16	4.10E-16
30	2.10E-15	7.45E-16	1.55E-15	8.20E-16	5.06E-16	5.25E-16	5.55E-16	4.30E-16	3.08E-16	4.20E-16
40	1.90E-15	6.40E-16	1.40E-15	7.50E-16	5.00E-16	5.15E-16	5.75E-16	4.05E-16	2.93E-16	4.10E-16
50	1.70E-15	5.70E-16	1.28E-15	6.50E-16	4.90E-16	4.90E-16	5.70E-16	3.70E-16	2.85E-16	3.90E-16
60	1.55E-15	5.10E-16	1.15E-15	5.80E-16	4.80E-16	4.60E-16	5.65E-16	3.40E-16	2.67E-16	3.70E-16
80	1.30E-15	4.25E-16	1.00E-15	4.70E-16	4.50E-16	4.15E-16	5.30E-16	2.95E-16	2.51E-16	3.25E-16
100	1.15E-15	3.50E-16	8.75E-16	4.00E-16	4.15E-16	3.70E-16	5.00E-16	2.60E-16	2.30E-16	2.80E-16
150	8.90E-16	2.70E-16	6.75E-16	3.05E-16	3.50E-16	3.10E-16	4.15E-16	2.00E-16	2.00E-16	2.30E-16
200	7.32E-16	2.20E-16	5.50E-16	2.35E-16	3.05E-16	2.70E-16	3.60E-16	1.60E-16	1.75E-16	1.95E-16
300	5.50E-16	1.70E-16	4.20E-16	1.80E-16	2.40E-16	2.10E-16	2.85E-16	1.25E-16	1.50E-16	1.45E-16
400	4.40E-16	1.35E-16	3.40E-16	1.40E-16	2.00E-16	1.70E-16	2.40E-16	1.00E-16	1.30E-16	1.20E-16
600	3.25E-16	9.80E-17	2.50E-16	1.05E-16	1.55E-16	1.27E-16	1.80E-16	7.30E-17	1.05E-16	9.00E-17
800	2.60E-16	7.60E-17	2.00E-16	8.30E-17	1.25E-16	1.05E-16	1.49E-16	5.80E-17	8.50E-17	7.30E-17
1000	2.18E-16	6.30E-17	1.65E-16	7.00E-17	1.07E-16	8.70E-17	1.25E-16	4.80E-17	7.30E-17	6.10E-17
2000	1.20E-16	3.40E-17	9.50E-17	3.90E-17	6.35E-17		7.50E-17	2.75E-17	4.40E-17	3.50E-17
4000	7.00E-17	1.90E-17	5.30E-17	2.20E-17	3.70E-17		4.35E-17	1.55E-17		2.00E-17
6000	5.00E-17	1.30E-17	3.80E-17	1.50E-17	2.60E-17		3.10E-17	1.10E-17		1.40E-17
10000	3.20E-17	8.30E-18	2.40E-17	1.00E-17	1.70E-17		2.05E-17	7.40E-18		9.00E-18

Table 2.6.8. Recommended cross sections for single-electron ionization of neutral atoms (Ga-Zr) under electron impact as a function of the electron impact energy (cf. Figs. 2.6.10 and 2.6.11).

Energy [eV]	Cross section [cm^2]								
	Ga	Ge	As	Se	Br	Kr	Rb	Sr	Zr
6							5.20E-16		
8	2.30E-16						8.00E-16	7.40E-16	3.90E-16
10	4.80E-16	1.00E-16					8.10E-16	9.80E-16	6.00E-16
15	8.60E-16	5.50E-16	2.80E-16	2.10E-16	1.05E-16	2.10E-17	7.60E-16	1.09E-15	8.10E-16
20	9.85E-16	6.30E-16	4.50E-16	3.80E-16	2.10E-16	1.20E-16	8.80E-16	1.05E-15	8.82E-16
25	1.05E-15	7.15E-16	5.50E-16	5.00E-16	3.10E-16	2.10E-16	9.30E-16	9.65E-16	8.92E-16
30	1.06E-15	7.30E-16	5.85E-16	5.40E-16	3.70E-16	2.60E-16	9.00E-16	8.85E-16	8.80E-16
40	1.03E-15	7.30E-16	6.20E-16	5.90E-16	4.30E-16	3.20E-16	8.30E-16	7.65E-16	8.18E-16
50	9.80E-16	7.20E-16	6.15E-16	5.90E-16	4.40E-16	3.40E-16	7.10E-16	6.65E-16	7.55E-16
60	9.15E-16	7.00E-16	5.95E-16	5.80E-16	4.40E-16	3.50E-16	6.30E-16	5.94E-16	6.95E-16
80	7.90E-16	6.35E-16	5.60E-16	5.55E-16	4.30E-16	3.50E-16	5.20E-16	4.94E-16	6.03E-16
100	6.90E-16	5.80E-16	5.25E-16	5.30E-16	4.05E-16	3.40E-16	4.60E-16	4.18E-16	5.23E-16
150	5.40E-16	4.60E-16	4.45E-16	4.60E-16	3.55E-16	3.20E-16	3.60E-16	3.00E-16	3.92E-16
200	4.50E-16	3.80E-16	3.98E-16	4.10E-16	3.10E-16	2.85E-16	3.10E-16	2.53E-16	3.34E-16
300	3.30E-16	2.75E-16		3.40E-16		2.35E-16	2.45E-16	1.87E-16	2.50E-16
400	2.80E-16	2.15E-16		3.00E-16		2.00E-16	2.10E-16	1.47E-16	2.01E-16
600	2.15E-16	1.60E-16		2.45E-16		1.45E-16	1.60E-16	1.08E-16	1.48E-16
800	1.80E-16	1.30E-16		2.05E-16		1.20E-16	1.40E-16	8.50E-17	1.15E-16
1000	1.50E-16	1.05E-16		1.75E-16		1.00E-16	1.25E-16	7.00E-17	9.60E-17
2000	9.00E-17	5.95E-17		1.07E-16		5.90E-17		4.00E-17	5.50E-17
4000		3.20E-17		5.90E-17		3.15E-17		2.20E-17	3.10E-17
6000		2.30E-17		4.20E-17		2.20E-17		1.60E-17	2.20E-17
10000		1.60E-17		2.90E-17		1.40E-17		1.00E-17	1.40E-17

Table 2.6.9. Recommended cross sections for single-electron ionization of neutral atoms (Mo-Xe) under electron impact as a function of the electron impact energy (cf. Figs. 2.6.12 and 2.6.13).

Energy [eV]	Cross section [cm^2]									
	Mo	Ru	Ag	Cd	In	Sn	Sb	Te	I	Xe
6					3.90E-17	8.00E-18	2.00E-18			
8	1.40E-16	9.00E-17	3.20E-17		2.00E-16	1.15E-16	5.20E-17			
10	3.50E-16	2.20E-16	1.05E-16	1.25E-16	4.20E-16	3.30E-16	1.95E-16	1.20E-16	4.00E-18	
15	6.30E-16	4.08E-16	2.00E-16	3.60E-16	7.00E-16	7.49E-16	5.70E-16	7.78E-16	1.90E-16	1.00E-16
20	7.18E-16	4.63E-16	2.60E-16	4.54E-16	7.00E-16	9.04E-16	7.26E-16	1.05E-15	3.82E-16	2.45E-16
25	7.46E-16	4.92E-16	2.90E-16	4.82E-16	6.80E-16	9.55E-16	8.10E-16	1.18E-15	4.90E-16	3.60E-16
30	7.53E-16	4.95E-16	3.00E-16	5.02E-16	6.60E-16	9.80E-16	8.30E-16	1.24E-15	5.53E-16	4.20E-16
40	7.56E-16	5.20E-16	3.00E-16	4.93E-16	6.60E-16	9.52E-16	8.10E-16	1.25E-15	6.00E-16	4.45E-16
50	7.37E-16	5.35E-16	2.90E-16	4.70E-16	7.00E-16	9.24E-16	7.85E-16	1.20E-15	5.96E-16	4.40E-16
60	7.16E-16	5.37E-16	2.70E-16	4.58E-16	7.50E-16	8.80E-16	7.60E-16	1.12E-15	5.90E-16	4.45E-16
80	6.56E-16	5.17E-16	2.60E-16	4.50E-16	8.00E-16	8.05E-16	7.20E-16	9.97E-16	5.85E-16	4.60E-16
100	6.05E-16	4.87E-16	2.60E-16	4.43E-16	7.90E-16	7.40E-16	6.70E-16	8.83E-16	5.55E-16	4.45E-16
150	4.80E-16	4.18E-16	2.35E-16	4.05E-16	7.00E-16	6.20E-16	5.70E-16	6.73E-16	4.70E-16	4.10E-16
200	4.18E-16	3.58E-16	2.10E-16	3.52E-16	6.30E-16	5.00E-16	4.50E-16	5.88E-16	4.10E-16	3.60E-16
300	3.27E-16	2.84E-16	1.65E-16	2.83E-16	5.20E-16			4.23E-16		2.90E-16
400	2.72E-16	2.34E-16	1.45E-16	2.38E-16	4.30E-16			3.42E-16		2.40E-16
600	2.05E-16	1.73E-16	1.05E-16	1.77E-16	3.40E-16			2.40E-16		1.80E-16
800	1.67E-16	1.33E-16	8.30E-17	1.44E-16	3.00E-16			1.98E-16		1.50E-16
1000	1.39E-16	1.16E-16	6.10E-17	1.20E-16	2.50E-16			1.60E-16		1.25E-16
2000	8.20E-17	6.70E-17		6.85E-17				9.30E-17		7.70E-17
4000	4.75E-17	3.80E-17		3.80E-17				5.20E-17		4.30E-17
6000	3.30E-17	2.60E-17		2.65E-17				3.80E-17		3.05E-17
10000	2.20E-17	1.75E-17		1.80E-17				2.40E-17		1.95E-17

Table 2.6.10. Recommended cross sections for single-electron ionization of neutral atoms (Cs-U) under electron impact as a function of the electron impact energy (cf. Figs. 2.6.14 and 2.6.15).

Energy [eV]	Cross section [cm^2]							
	Cs	Ba	Au	Hg	Tl	Pb	Bi	U
6	3.60E-16	4.00E-16					2.50E-17	
8	6.30E-16	1.25E-15			1.60E-16	1.05E-16	1.60E-16	1.40E-16
10	7.80E-16	1.45E-15			2.60E-16	2.10E-16	3.36E-16	1.90E-16
15	9.20E-16	1.25E-15		1.75E-16	4.10E-16	4.10E-16	6.25E-16	3.40E-16
20	8.30E-16	1.45E-15		3.30E-16	4.50E-16	5.20E-16	7.61E-16	4.35E-16
25	9.20E-16	1.40E-15		4.40E-16	4.80E-16	6.00E-16	8.40E-16	4.80E-16
30	9.35E-16	1.25E-15		5.00E-16	5.30E-16	6.20E-16	8.73E-16	5.00E-16
40	9.30E-16	1.00E-15		5.60E-16	6.10E-16	6.00E-16	8.75E-16	4.70E-16
50	9.00E-16	8.40E-16	1.15E-15	5.80E-16	6.60E-16	5.80E-16	8.61E-16	4.30E-16
60	8.40E-16	7.30E-16	1.40E-15	5.70E-16	6.90E-16	5.60E-16	8.20E-16	3.90E-16
80	7.80E-16	5.90E-16	1.45E-15	5.40E-16	7.25E-16	5.00E-16	7.75E-16	3.45E-16
100	7.10E-16	4.80E-16	1.40E-15	5.00E-16	7.20E-16	4.35E-16	7.40E-16	3.15E-16
150	5.80E-16	3.30E-16	1.25E-15	4.20E-16	6.60E-16	3.50E-16	6.20E-16	2.60E-16
200	5.20E-16	2.55E-16	1.15E-15	3.50E-16	5.85E-16	3.05E-16	5.10E-16	2.30E-16
300	4.20E-16	1.80E-16	9.60E-16	2.70E-16	4.60E-16	2.45E-16		1.90E-16
400	3.50E-16	1.35E-16	8.50E-16	2.30E-16	3.80E-16	2.10E-16		1.70E-16
600	2.80E-16	1.00E-16	7.30E-16	1.75E-16	2.90E-16	1.75E-16		1.45E-16
800	2.35E-16	7.50E-17	6.30E-16	1.45E-16	2.30E-16	1.50E-16		1.25E-16
1000	2.10E-16	6.20E-17	5.60E-16	1.30E-16	1.95E-16	1.35E-16		1.15E-16

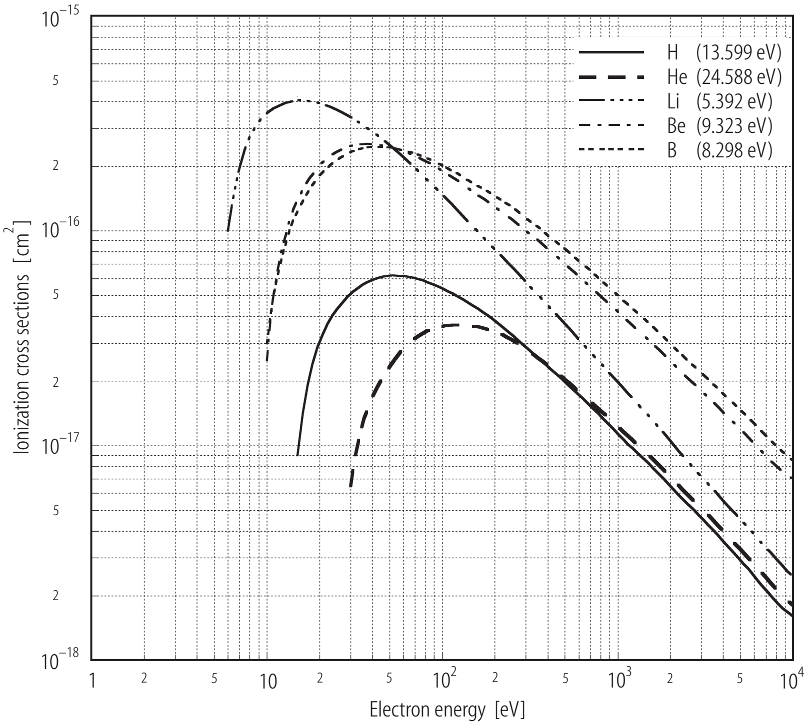

Fig. 2.6.4. Single-electron ionization cross sections for hydrogen to boron atom plotted as a function of electron impact energy (cf. Table 2.6.5).

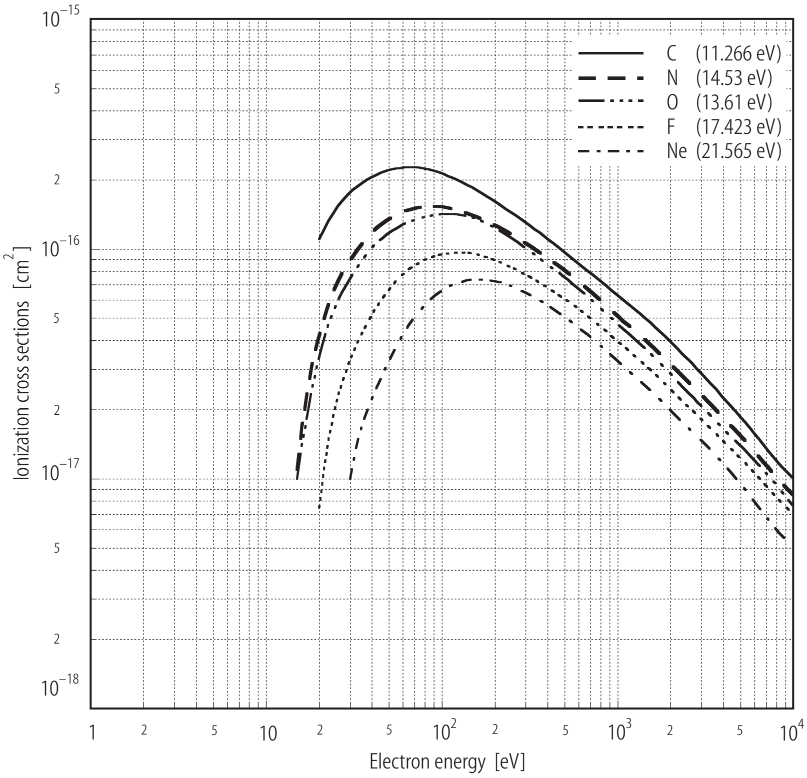

Fig. 2.6.5. Single-electron ionization cross sections for carbon to neon atom plotted as a function of electron impact energy (cf. Table 2.6.5).

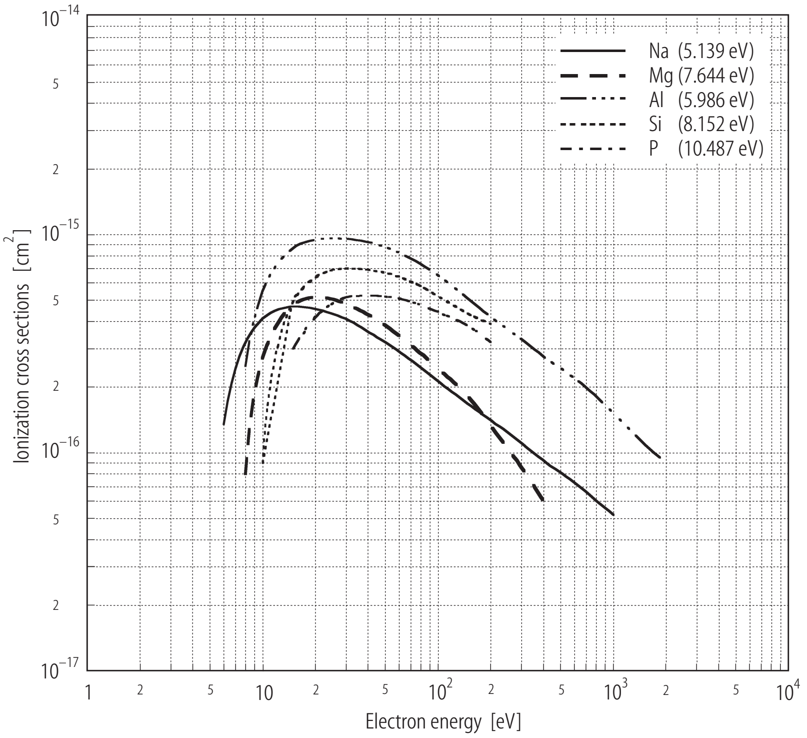

Fig. 2.6.6. Single-electron ionization cross sections for sodium to phosphor atom plotted as a function of electron impact energy (cf. Table 2.6.6).

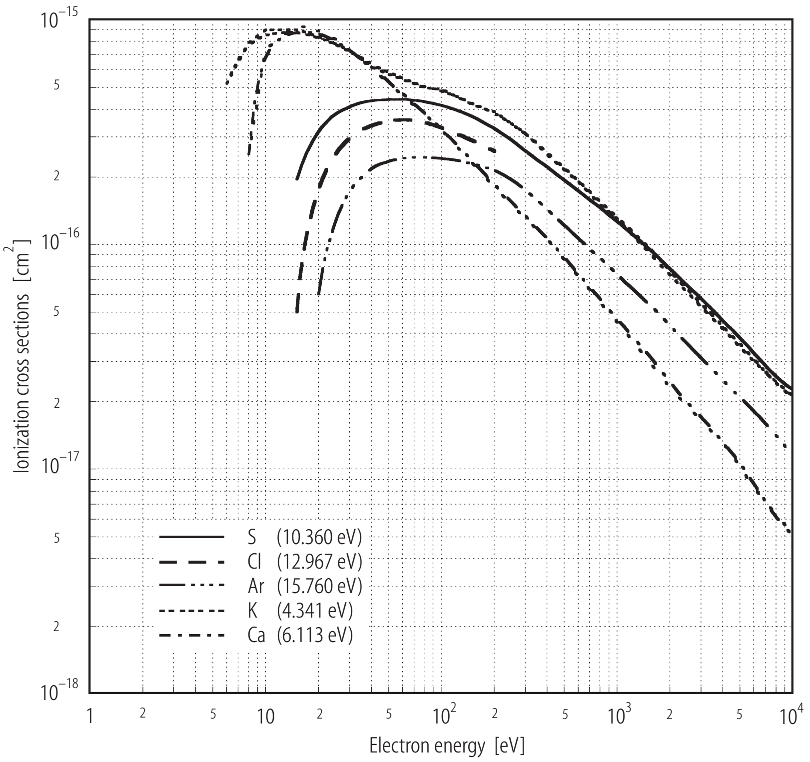

Fig. 2.6.7. Single-electron ionization cross sections for sulfur to calcium atom plotted as a function of electron impact energy (cf. Table 2.6.6).

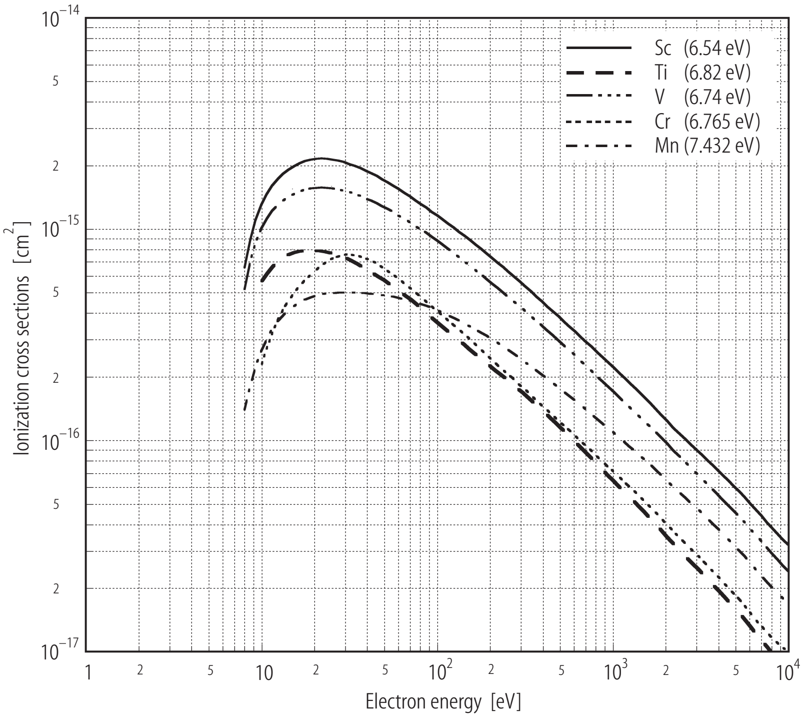

Fig. 2.6.8. Single-electron ionization cross sections for scandium to manganese atom plotted as a function of electron impact energy (cf. Table 2.6.7).

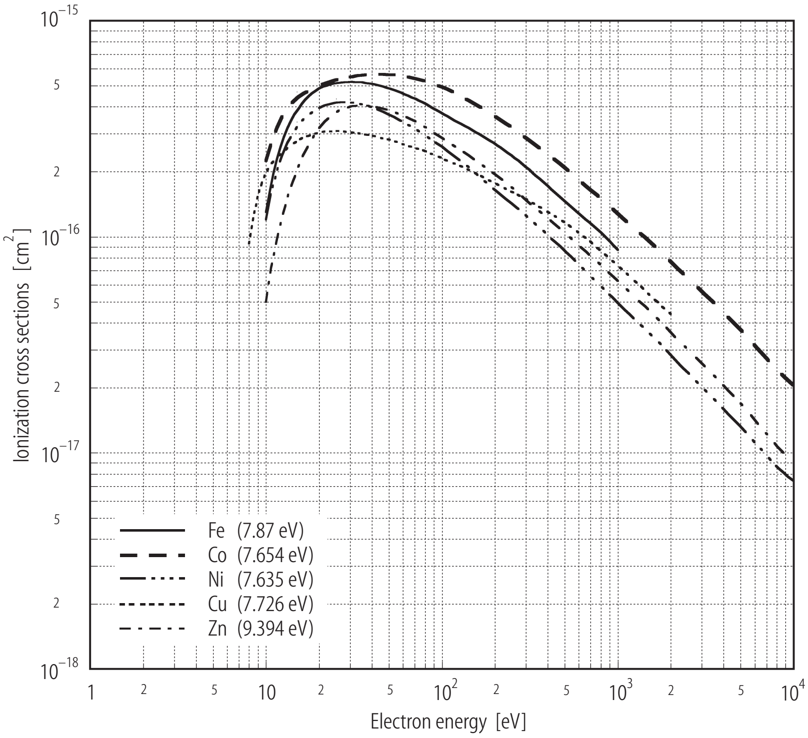

Fig. 2.6.9. Single-electron ionization cross sections for iron to zinc atom plotted as a function of electron impact energy (cf. Table 2.6.7).

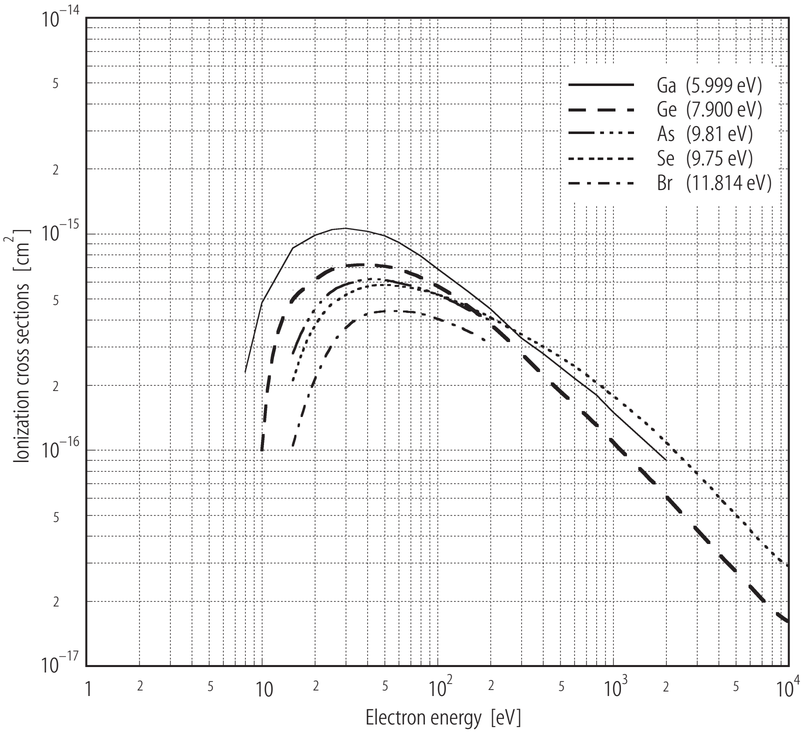

Fig. 2.6.10. Single-electron ionization cross sections for gallium to bromine atom plotted as a function of electron impact energy (cf. Table 2.6.8).

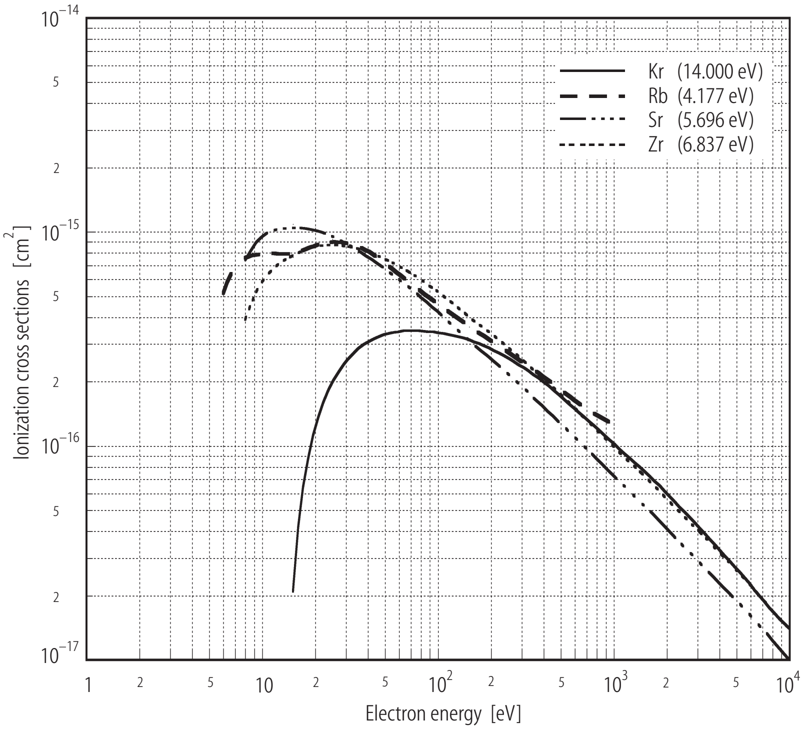

Fig. 2.6.11. Single-electron ionization cross sections for krypton to zirconium atom plotted as a function of electron impact energy (cf. Table 2.6.8).

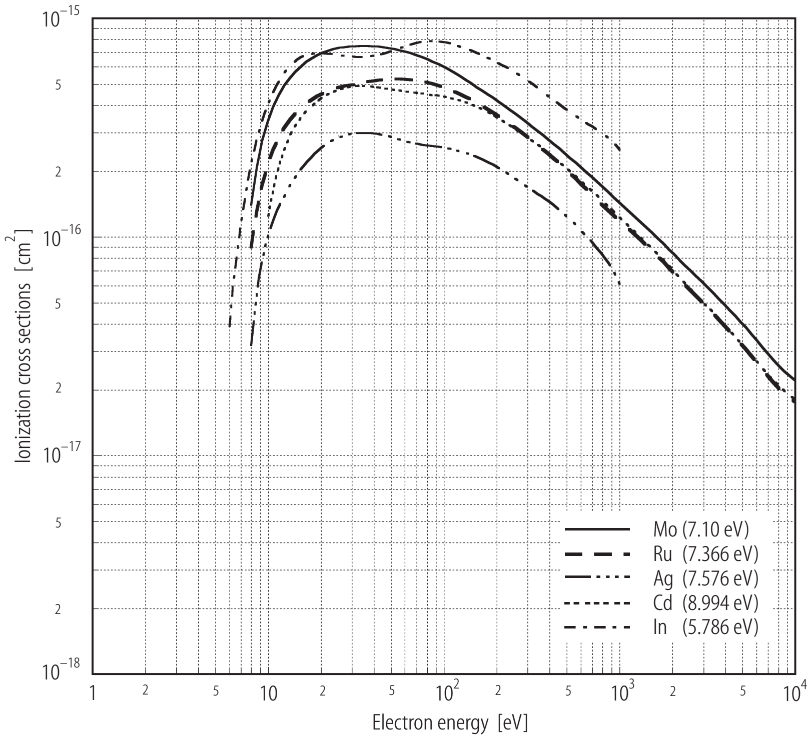

Fig. 2.6.12. Single-electron ionization cross sections for molybdenum to indium atom plotted as a function of electron impact energy (cf. Table 2.6.9).

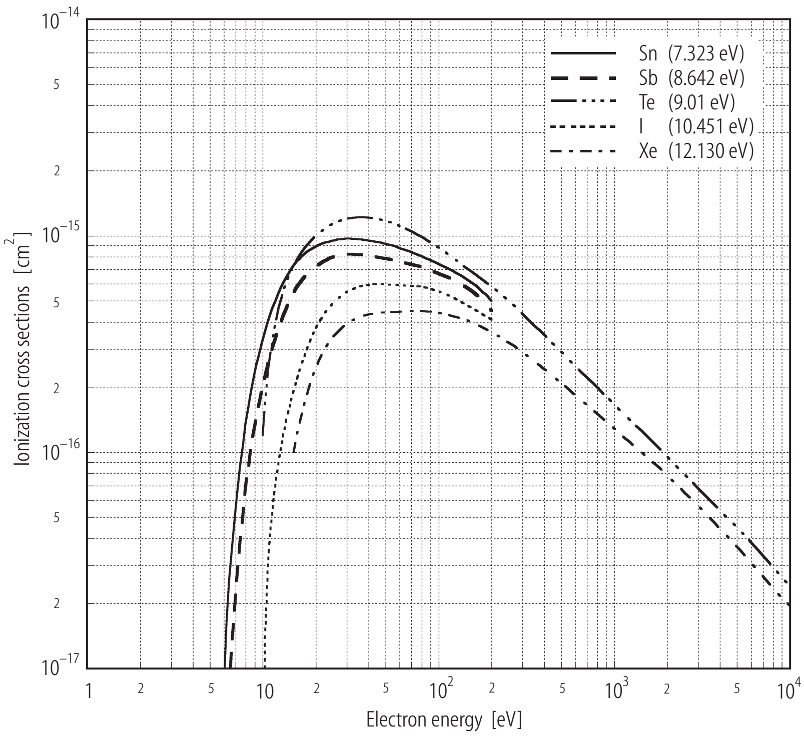

Fig. 2.6.13. Single-electron ionization cross sections for tin to xenon atom plotted as a function of electron impact energy (cf. Table 2.6.9).

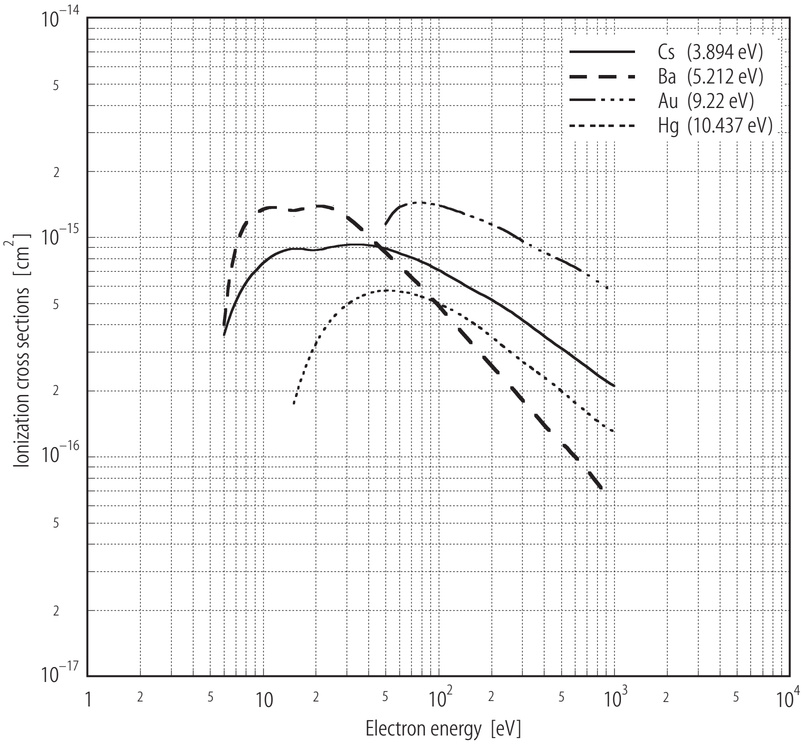

Fig. 2.6.14. Single-electron ionization cross sections for cesium to mercury atom plotted as a function of electron impact energy (cf. Table 2.6.10).

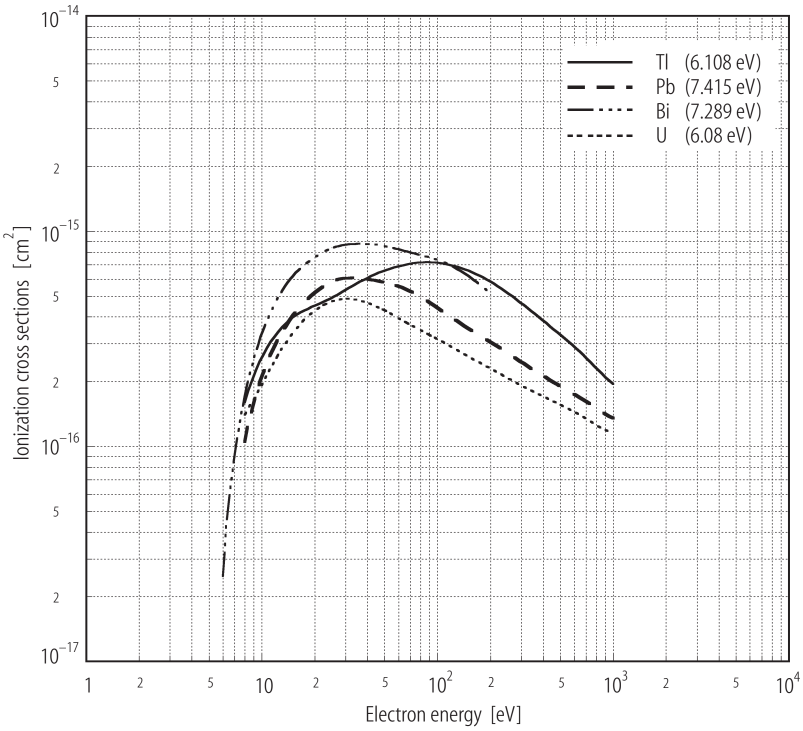

Fig. 2.6.15. Single-electron ionization cross sections for thallium to uranium atom plotted as a function of electron impact energy (cf. Table 2.6.10).

2.6.5 Short description of theories

The theories for the electron impact direct ionization have been developed for quite some time. A number of different approximation methods have been used [85Mär1].

One of the most significant progresses in theories of ionization under electron impact in recent years is the development of the convergent close-coupling (CCC) method which has been found to be very powerful and accurate not only in the ground state species but also in the excited species [92Bra1, 93Bra1]. Now realizing such progresses in theories, new and more accurate experiments are urgently required.

2.6.6 Empirical formula for ionization cross sections for outer-shell electrons

In a number of applications, it is important to have some empirical formulas to get the ionization cross sections under electron impact. So far, many basically identical but slightly different empirical formulas have been proposed [85Mär1]. There are also some critical reviews on the existing empirical formulas. Some of them are found to be convenient in many uses.

2.6.6.1 Empirical formulas for single ionization

One of the most familiar and convenient forms had been proposed by Lotz [67Lot1, 68Lot1] many years ago and is still widely in use in a number of cases. The total ionization cross sections are given as the sum of the contribution from different (sub-) shells as follows:

$$\sigma_{\mathrm{i}} = \sum_j a_j N_j \frac{\ln(u)}{u I_j^2}\left[1 - b_j \mathrm{e}^{-c_j(u-1)}\right] \qquad (3)$$

where I_j is the ionization threshold energy of the j-th shell electron, the reduced electron energy $u = E/I_j$, E being the electron incident energy, N_j the number of the electrons in the j-th shell and a_j, b_j and c_j constants given for different shells [67Lot1, 68Lot1]. The total cross sections have to be summed up over all the possible j-th shells. This empirical formula is known to work surprisingly nicely even for neutral target atoms where the direct ionization processes are dominant over the indirect ionization processes (see Section 3.2 for ionization of ions).

Extensive survey of the electron ionization cross section data shows another simple analytical expression as follows:

$$\sigma_{\mathrm{i}} = \frac{1}{u I_j^2}\left[a \ln(u) + \sum_n b_n \left(1 - \frac{1}{u}\right)^n\right] \qquad (4)$$

where the parameters are the same as in eq. (3) and a and b_n constants. These constants are given in [83Bel1, 88Len1, 89Hig1] for most of the neutral species (as well as typical charge state ions) of H to U. Also the number of the terms, n, which is necessary to get the best fit to the experimental data, does depend on the target species and are given [83Bel1, 88Len1, 89Hig1]. It should be, however, noted that artificial oscillations of the cross sections are sometimes seen in this type of the fitting when they are plotted as a function of the electron energy [97God1].

Empirical formula with relatively simple but physically clear background based upon the binary-encounter-dipole (BED) model has been recently discussed [94Kim1]. This formula, without requiring any fitting parameters, show a reasonable agreement with the experimental data for one-electron atoms (and ions, too). After comparing this theoretical formula with the data available, the following empirical formula based upon the BED has been proposed:

$$\sigma_{\mathrm{i}} = \frac{3.52}{u}\left[a\ln(u) + b\left(1-\frac{1}{u}\right) + c\frac{\ln(u)}{u+1}\right] \tag{5}$$

where a, b and c are the fitting parameters.

It should be pointed out that this basic empirical formula based upon BED can provide not only the total ionization cross sections but also the differential (angular and energy) cross sections of the secondary electrons which are found to be in reasonable agreement with the experiments.

Another convenient empirical formula of the single-electron ionization cross sections based upon the semiclassical approach has recently been proposed for neutral atoms ranging from hydrogen to uranium atoms [94Mar1]. The following formula for the partial ionization cross section of the sub-shell with the quantum numbers (nl) is given:

$$\sigma_{\mathrm{i}}^{j} = \pi r_j^2 g_j N_j f(u) \tag{6}$$

where r_j is the electron orbital radius of the j-th shell which is quantum-mechanically calculated, g_j the weighting factor for different shells, N_j the number of electrons in the j-th shell and the energy-dependent universal function $f(u)$ has the following form:

$$f(u) = \left(\frac{u-1}{u+1}\right)^{a}\frac{1}{u}\left(b + c\left\{1-\frac{1}{2u}\right\}\ln\left\{2.7+(u-1)^{1/2}\right\}\right) \tag{7}$$

with $u = E/I_j$, E and I_j representing the incident electron energy and the binding energy of the j-th shell, respectively. It has been found that, in order to get better fit to the experimental data, the constants a, b and c are varied for different shells, namely a = 7/4, b = 1, c = 1 for s-shell; a = 2, b = 1, c = 1 for p-shell; a = 3/2, b = 3, c = 2/3 for d-shell and a = 3/2, b = 1, c = 2/3 for f-shell and the factors for different shells are given [94Mar1]. Finally the total single electron ionization cross sections are given as follows:

$$\sigma_{\mathrm{i}} = \sum_j \sigma_{\mathrm{i}}^{j} \tag{8}$$

This formula has been found to be in generally good agreement with the experimental data within ± 10 % for most of the neutral species up to U and within ± 30 % for a few neutrals.

2.6.6.2 Analytical and empirical formula for ionization of inner-shell electrons

There are ab initio relativistic calculations of the inner-shell electron ionization by relativistic electron impact which show good agreement with the experimental results [78Sco1]. Yet sometimes, it is convenient to have simpler expressions for the innershell-electron ionization by the relativistic electrons.

It is well known that the relativistic collision processes can be nicely described through the Weizsacker-William method based upon the virtual photon interactions due to the electro-magnetic field generated by the passing high velocity charged particles. One of the simplest analytical formulas for total ionization cross sections [67Kol1] has been found to be in good agreement with a number of the observed data [70Mid1, 77Ish1]. The cross sections (in units of 10^{-24} cm^2) are given as the sum of two parts, namely the distant collisions (due to the virtual photon; $\sigma_{\mathrm{i}}^{\mathrm{d}}$) and close collisions (due to Coulomb interaction; $\sigma_{\mathrm{i}}^{\mathrm{c}}$):

$$\sigma_{\mathrm{i}}^{\mathrm{d}} = \frac{0.275}{I_j}\frac{(E+1)^2}{E(E+2)}\left[\ln\left\{\frac{1.19E(E+2)}{I_j}\right\} - \frac{E(E+2)}{(E+1)^2}\right] \text{ barn} \tag{9}$$

$$\sigma_{\rm i}^{\rm c} = \frac{0.99}{I_j}\frac{(E+1)^2}{E(E+2)}\left[1-\frac{E}{I_j}\left\{1-\frac{E^2}{2(E+1)^2}+\frac{2E+1}{(E+1)^2}\ln\left(\frac{E}{I_j}\right)\right\}\right] \text{ barn} \tag{10}$$

Here E and I_j represent the kinetic energy of the incident electrons and the ionization energy of the j-th inner-shell, both in the units of the electron rest mass energy (m_0c^2 where m_0 and c represent the electron rest mass and the velocity of light), respectively. It can be noted that the calculated ionization cross sections of the relativistic electrons in heavy H-like ions such U^{91+} ions are also found to be in agreement within a factor of two with those recently observed near the threshold region (see Section 3.2).

It should be pointed out that the differential cross sections of the secondary electrons caused by the inner-shell ionization have been nicely given based upon the virtual photon interactions [90May1], combined with the Møller interactions.

There is another work to find some empirical formula relevant to the ionization of the inner-shell (K, L and M) target electrons including the sub-shell electrons at the relativistic electron impact [94Deu1]. In principle, this empirical formula is the same as that given in eqs. (6)-(8), with the additional relativistic corrections. Thus the ionization cross sections are given as follows:

$$\sigma_{\rm i}^{j} = \pi r_j^2 g_j N_j\, f(u) F(u) \tag{11}$$

where $F(u) = R(1 + 2u^{1/4}/J^2)$ with $J = m_0c^2/I_j$, m_0c^2 being the electron rest mass energy. R, another relativistic correction factor, is given as a function of u and J [65Gry1]. Other parameters are the same as those given in eq. (6). The weighting factors g_j for K-, L- and M-(sub)shells are also given. The agreement with the experimental data is reasonable but the deviation has been clearly seen at high energies.

2.6.6.3 Empirical formula for multiple ionization of neutral atoms

Multiple electron ionization processes are much more complicated but they have been investigated to some extent [87Taw1]. It is not easy to find simple empirical formulas, even for the double-electron ionization cross sections, as many electron atoms are expected to have the significant but different contribution from the indirect processes which are not easily formulated. Yet there are some proposals to formulate such multiple electron ionizations.

One recently proposed analytical formula [95She1, 97Bél1] for m-times ($m \geq 2$) electron ionization, based upon analysis of the experimental data available, is given as follows, under the condition that the indirect processes are not significant, meaning that the empirical formula is better fitted with the observations at relatively high energies (in units of 10^{-18} cm^2):

$$\sigma_{m{\rm i}} = \frac{aN^b}{I_m^2}\frac{u-1}{u}\frac{\ln u}{u} \tag{12}$$

where I_m represents the threshold energy for removal of the m outer-most electrons (in Rydberg units) and is given as

$$I_m = \sum_{j}^{m-1} I_{j,j+1} \ ,$$

$I_{j,\,j+1}$ being the single-electron ionization energy from the charge j to j+1, $u = E/I_m$, E being the incident energy of electrons (in Rydberg units), N the total number of electrons in a target atom and a and b constants and given in Table 2.6.11, depending on the number of the electrons to be ionized, m. It has been found that this can provide reasonable agreement (within a factor of two) with the experimental data for multiple-electron ionization up to 13 electrons.

Table 2.6.11. Constants in empirical formula (eq. (12)) for multiple-electron ($m \geq 2$) ionization.

m	a	b
2	14.0	1.08
3	6.30	1.20
4	0.50	1.73
5	0.140	1.85
6	0.049	1.96
7	0.021	2.00
8	0.0096	2.00
9	0.0049	2.00
10	0.0027	2.00

For $m > 10$, the following asymptotic form can be used:

$$a\,(m > 10) \approx 1350\, m^{-5.7}$$
$$b\,(m > 10) \approx 2.00. \qquad (13)$$

Another semiclassical formula [96Deu1] has also been proposed based upon the procedures described before. To get the cross sections of the m-electron ionization, the single ionization formula has to be summed over the contributing sub-shells:

$$\sigma_{m\mathrm{i}} = g^m \sum_k \pi r_k^2 N_k f_k(u) \qquad (14)$$

where r_k represents the mean-electron radius of the k-th sub-shell (k = 1 referring to the outermost shell, etc.), N_k the number of electrons in the k-th sub-shell and $f_k(u)$ the universal function depending upon the shell given before (see eq. (7)). g^m is the weighting factor which has been estimated from the experimental data available and has been found to be strongly dependent on the nuclear charge of the target species. So far, this formula has been shown to be in reasonable agreement with the multiple-electron ionization up to m = 5.

One more example of the empirical formulas for m-multiple electron ionization, based upon the well-understood formula, combining with some statistical consideration is given recently [95Fis1] as follows (in units of 10^{-16} cm^2):

$$\sigma_{m\mathrm{i}} = \frac{3.52}{17^{m-1}} \frac{\zeta_m}{I_m^2} \left(1 - 2e^{-0.7u}\right) u^{-1.4} \ln(u) \qquad (15)$$

where the minimum energy for removing m-electrons I_m is given in Rydberg units and ζ_m the statistical factor which depends slightly on whether m electrons are removed from the single outermost or the two more shells. It should be noted that this is not valid near the threshold where another treatment is necessary. Generally the agreement with the experimental data seems to be reasonable up to m = 7.

2.6.6.4 Ionization rate coefficients

So-called ionization rate coefficients, which are averaged over some distributions of the electron energy or temperatures such as the Maxwellian distributions, are also useful, particularly in applications involving basic and industrial plasmas [83Bel1, 88Len1, 89Hig1]. But it has been recently realized that the original cross section data are more convenient in many applications and indeed there are a number of cases which do not follow the Maxwellian distributions and another procedure is necessary to get the rate coefficients for different energy distributions.

A number of different empirical forms for the ionization rate coefficients, namely the cross sections multiplied by the electron velocity, <$\sigma_i v_e$>, averaged over the Maxwellian velocity (temperature) distributions have been proposed.

1. One of the most commonly used forms is represented in the following [83Bel1, 88Len1, 89Hig1]:

$$\langle \sigma_i v_e \rangle = \mathrm{e}^{-I_i/kT} \left(\frac{kT}{I_i} \right)^{1/2} \sum \alpha_n \left(\log \frac{kT}{I_i} \right)^n \qquad \text{for } I_i/10 \le kT \le 10 I_i \qquad (16a)$$

$$\langle \sigma_i v_e \rangle = \left(\frac{kT}{I_i} \right)^{-1/2} \left\{ \gamma \ln \frac{kT}{I_i} + \sum \beta_n \left(\frac{I_i}{kT} \right)^n \right\} \qquad \text{for } kT > 10 I_i \qquad (16b)$$

where I_i and T represent the ionization energy of ion and the electron temperature, respectively. The parameters, α_n, β_n,and γ, are given in the references for a number of atoms in various ionization [83Bel1, 88Len1, 89Hig1].

2. Based upon the recommended ionization data [83Bel1, 88Len1, 89Hig1] from H to Ni neutral atoms, another simple fitting formula for ionization rate coefficients has been recently proposed,

$$\langle \sigma_i v_e \rangle = a\left(1 + P u^{1/2}\right) u^k \frac{e^{-u}}{X + u} \qquad (17)$$

where $u = I_i/T$, I_i is the ionization energy of ions and T the electron temperature. a, k and X are the adjustable parameters which have been determined from the best fit to the recommended data. P is another adjustable parameter to fit the threshold behavior (in most cases P is 0 or 1). These parameters are given in the reference [97Vor1].

Acknowledgement

The present author would like to thank Dr. I.Murakami, Mr. T.Imai and Mr. M.Kato of NIFS for their help in making some figures and tables used here.

2.6.7 References for 2.6

65Gry1 Gryzinski, M.: Phys. Rev. **138** (1965) 322.
67Kol1 Kolbenstvedt, H.: J. Appl. Phys. **18** (1967) 4785.
67Lot1 Lotz, W.: Z. Phys. **206** (1967) 205.
68Lot1 Lotz, W.: Z. Phys. **216** (1968) 241.
70Mid1 Middleman, L.M., Ford, R.L., Hofstadter, R.: Phys. Rev. A **2** (1970) 1429.
71Ino1 Inokuti, M.: Rev. Mod. Phys. **43** (1971) 297.
77Ish1 Ishii, K., Kamiya, M., Sera, K., Morita, S., Tawara, H., Oyamada, M., Chu, T.C.: Phys. Rev. A **15** (1977) 906.
78Sco1 Scofield, J.H.: Phys. Rev. A **18** (1978) 963.
83Bel1 Bell, K.L., Gilbody, H.B., Hughes, J.G., Kingston, A.E., Smith, F.J.: J. Phys. Chem. Ref. Data **12** (1983) 891.
85Mär1 Märk, T.D., Dunn, G.H.: Electron Impact Ionization, Wien, New York: Springer 1985.
85Pow1 Powell, C.J.: in [85Mär1], p. 198.

86Be1 Be, S.H., Tonuma, T., Kumagai, H., Shibata, H., Kase, M., Kambara, T., Kohno, I., Tawara, H.: J. Phys. B **19** (1986) 1771.
87Sha1 Shah, M.B., Elliot, D.S., Gilbody, H.B.: J. Phys. B **20** (1987) 3501.
87Taw1 Tawara, H., Kato, T.: At. Data Nucl. Data Tables **36** (1987) 167; Tawara, H., Kato, M. NIFS-Data 51 (1999).
88Len1 Lennon, M.A., Bell, K.L., Gilbody, H.B., Hughes, J.G., Kingston, A.E., Murray, M.J., Smith, F.J.: J. Phys. Chem. Ref. Data **17** (1988) 1285.
89Hig1 Higgins, M.J., Lennon, M.A., Hughes, J.G., Bell, K.L., Gilbody, H.B., Kingston, A.E., Smith, F.J.: CLM-R294, Culham Laboratory, UK, 1989.
90Lon1 Long, X., Liu, M., Ho, F., Peng, X.: At. Data Nucl. Data Tables **45** (1990) 353.
90May1 Mayol, R., Salvat, F.: J. Phys. B **23** (1990) 2117.
92Bra1 Bray, I., Stelbovics, A.T.: Phys. Rev. A **46** (1992) 6995.
92Tra1 Trajmar, S., Nickel, J.C.: Adv. At. Mol. Opt. Phys. **30** (1992) 45.
93Bra1 Bray, I., Stelbovics, A.T.: Phys. Rev. Lett. **70** (1993) 746.
93Gie1 Gieler, M., Aumayr, F., Schweinzer, J., Koppensteiner, W., Husinsky, W., Winter, HP., Lozkina, K., Hansen, J.P.: J. Phys. B **26** (1993) 2137.
93Ric1 Richter, C., Andersen, N., Benoit, J.C., Dowek, D., Houver, J.C., Salgado, L., Thomsen, T.W.: J. Phys. B **26** (1993) 723.
94Deu1 Deutsch, H., Margreiter, D., Märk, T.D.: Z. Phys. D **29** (1994) 31.
94Kim1 Kim, Y.K., Rudd, M.E.: Phys. Rev. A **50** (1994) 3954.
94Mar1 Margreiter, D., Deutsch, H., Märk, T.D.: Int. J. Mass Spectrom. Ion Process **139** (1994) 127.
95DeP1 DePaola, B., Huang, M.T., Winecki, S., Kanai, Y, Lundeen, S.R., Fehrenbach, C.W., Arko, S.A.: Phys. Rev. A **52** (1995) 2136.
95Fis1 Fisher, V., Ralchenko, Yu., Goldgirsh, A., Fisher, D., Martin, Y.: J. Phys. B **28** (1995) 3027.
95She1 Shevelko, V.P., Tawara, H.: J. Phys. B **28** (1995) L589.
96Deu1 Deutsch, H., Becker, K., Märk, T.D.: J. Phys. B **29** (1996) L497.
96Sch1 Schappe, R.S., Walker, T., Anderson, L.W., Lin, C.C.: Phys. Rev. Lett. **76** (1996) 4328.
96Tan1 Tan, W.S., Shin, Z., Ying, C.H., Vuskovic, L.: Phys. Rev. A **54** (1996) R3710.
97Bél1 Bélenger, C., Defrance, P., Salzborn, E., Shevelko, V.P., Tawara, H., Uskov, D.B.: J. Phys. B **30** (1997) 2667.
97Dep1 Depaola, B.: Accelerator-Based Atomic Physics Techniques and Applications (S. Shafroth, J.A. Austin, eds.), American Institute of Physics (1997), p. 677.
97God1 Godunov, A.: Abstract Book, International Conference on Physics of Electronic and Ionic Collisions (F. Aumayr, G. Betz, HP. Winter, eds.), (1997), p.TU199 and private communication (1997).
97Taw1 Tawara, H.: AIP Proceedings of International Conference on Atomic Molecular Data and Their Applications (W. Wiese, ed.), in printing, Gaithersburg, USA, (1997), p.434.
97Vor1 Voronov, G.S.: At. Data Nucl. Data Tables **65** (1997) 1.
www1 www at http://dbshino.nifs.ac.jp (accessible after getting the ID) (National Institute for Fusion Science, Toki, Japan).
www2 www at http://wwwndc.tokai.jaeri.go.jp/JEAMDL/index.html (Japan Energy Research Institute, Tokai, Japan).
www3 www at http://ornl.gov (Oak Ridge National Laboratory, Oak Ridge, TN, USA).
www4 www at http://iaea.org.at (International Atomic Energy Agency, Wien, Austria).